

# Peripheral Organ Dose Evaluation using a Human Body Phantom in Intensity Modulated Radiation Therapy for Lung Cancer with Helical Type Accelerator

Shinichi GOTOH,<sup>1</sup> Yasuhiro KAWAHARADA,<sup>2</sup> Satoshi SUDA,<sup>3</sup> Masataka UETANI<sup>1</sup>

<sup>1</sup>Department of Radiological Sciences, Nagasaki University Graduate School of Biomedical Sciences, 1-7-1 Sakamoto, Nagasaki 852-8501, Japan

<sup>2</sup>Department of Radiological Technology, Gunma Prefectural College of Health Sciences, 323-1 Kamioki-cho, Maebashi-shi, Gunma 371-0052, Japan

<sup>3</sup>Oncology Center of Hidaka Hospital, 886 Nakao-cyo, Takasaki-shi, Gunma 370-0001, Japan

**Purpose:** Intensity modulated radiation therapy (IMRT) is characterized by a relatively long period for beam exposure and consequently the risk for unnecessary exposure to non-targeted organs, mainly due to the scattered radiation, should be considered. The purposes of this study are to measure the absorbed dose of the peripheral organs during helical IMRT using a fluorescent glass dosimeter.

**Materials and Methods:** In this research, we took lung cancer as a model and measured the absorbed dose of the peripheral organs during helical IMRT using a fluorescent glass dosimeter. The planning target volume (PTV) dose of 95% was set to be 5 Gy in the phantom.

**Results and Discussion:** The highest exposure dose was observed for the breasts, which were on the PTV trajectory, with the left and right breasts receiving doses of 227.94 mGy and 371.90 mGy, respectively. The exposure doses of the left and right lenses were 3.13 mGy for the left lens and 3.22 mGy for the right lens. An exponential dose reduction to the distance from PTV was confirmed. Our data suggest that the doses for peripheral organs were acceptable in lung cancer case based on past literature search. However, the use of custom blocks for the eyes should be considered to prevent possible late occurrence of cataract.

ACTA MEDICA NAGASAKIENSIA 55: 61 - 67, 2011

**Keywords:** helical tomotherapy, intensity modulated radiation therapy, peripheral organ dose, glass dosimeter

## Introduction

Intensity modulated radiation therapy (IMRT) is a treatment that concentrates a radiation dosage in a target volume<sup>1</sup>. The normal tissue dose can be reduced to the greatest extent by optimization calculations according to the treatment plan<sup>2</sup>. Simulations need to be performed to investigate the effect of secondary radiation on these optimization calculations, with corrections based on differences in penetrated organ density. For this purpose, highly complex calculations and verification experiments using a phantom are

necessary prior to the treatment by a method called inverse planning<sup>3</sup>.

The exposure time in IMRT (150 to 300 seconds or more) is generally longer than that in conventional radiation therapy because IMRT employs many narrow photon beams<sup>7</sup>. Moreover, according to the algorithm used for the optimization calculations, the dose in the vicinity of the body surface, such as the breasts and eyes is affected by factors such as the airspace surrounding the body; thus, the optimized calculation value for the treatment plan and the actual absorbed dose might not be in agreement. The likelihood of

**Address correspondence:** Department of Radiological Sciences, Nagasaki University Graduate School of Biomedical Science, 1-7-1 Sakamoto, Nagasaki 852-8501, Japan

TEL: +81-03-3816-2129, FAX: +81-03-5803-1990, E-mail: goto-ngs@umin.ac.jp

Received February 2, 2010; Accepted November 30, 2010

errors is especially high in the low-dose region because the measurement performance of the ionization chamber detector is relatively poor at such doses.

The purpose of this study is to measure the absorbed dose of the risk organs during helical tomotherapy IMRT using a fluorescent glass dosimeter.

## Materials and Methods

### *Helical Tomotherapy*

Helical tomotherapy is one of the most advanced IMRT equipment, which has computerized tomography (CT) based helical type exposure functions<sup>4-6</sup>. In this system, radiation therapy is executed as the couch moves through the gantry, which rotates in the same manner as a CT apparatus for diagnostic use. The beam used for exposure is a slit shaped narrow beam called a beamlet. As the apparatus rotates, the beam is modulated with exposure time, and thereby IMRT can be effectively performed<sup>9-11</sup>. We employed TomoTherapy Hi-Art System (TomoTherapy, Wisconsin, USA) for helical tomotherapy. The treatment beam energy was applied via a 6 MV convex beam without use of a flattening filter. The radiation source to isocenter separation was 85 cm and the maximum irradiation field was  $5 \times 40 \text{ cm}^2$  at the isocenter.

### *Fluorescent Glass Dosimeter*

The beam generated in helical tomotherapy is a slit narrow beam, which can be as small as  $0.6 \times 1.25 \text{ cm}^2$ . For this reason, we used a fluorescent glass dosimeter, which is suitable for measurements in the low-dose region for extremely narrow beams<sup>8</sup>. A glass dosimeter (Asahi Glass, Jpn) was used to measure the absorbed dose values in various parts of the phantom (RAN-100, THE PHANTOM LABORATORIES, INC., USA) (Fig.1). This apparatus utilizes radiophotoluminescence, a luminescent phenomenon which occurs when certain types of glass are struck by ultraviolet rays after exposure to radiation. Fluorescent glass dosimeters exploit the chemical transition of silver ions in silver-activated phosphate glass; because the fluorescence center produced by the divalent silver ion ( $\text{Ag}^{2+}$ ) or silver particles ( $\text{Ag}^0$ ) due to the radiation is exceedingly stable, the loss of dose information, called fading, is extremely small at less than 1% per year. Moreover, as the fluorescence center does not vanish when measured and can be repeatedly read many times, the statistical accuracy of the measurements is enhanced and a stable measurement value can be acquired<sup>12,13</sup>. We used GD-352 for the phosphate



**Fig. 1.** Human body Rando-phantom on the Helical type accelerator treatment couch.

glass element. In addition, we used it as a bare element without an additional filter for low energy and calibrated it with 6MV X-ray. As a result, the calibration constant we obtained was 1.16.

### *Experimental Measurements*

We carried out absorbed dose measurements by establishing a virtual target in the chest of a human-body phantom. Measurements were carried out at the locations corresponding to the left and right breasts on the exposure trajectory and at locations corresponding to the thyroid, pelvic region, and left and right crystalline lenses outside the exposure trajectory. We calibrated each detection element of the fluorescent glass dosimeter by using a standardized linear accelerator. Exposure was carried out with an irradiation field of  $15 \text{ cm} \times 15 \text{ cm}$  and a radiation source to ionization chamber detector separation of 100 cm according to the 6 MV X-rays acquired from a standard linear accelerator (Varian Torilogy, USA). A conventional standard ionization chamber was used in this study (M30013, PTW, Germany).

For the treatment plan, we adopted a right lung cancer as a model and set the PTV at 15 cm below the thyroid gland (Fig.2). We assumed spheres of 2 cm in diameter for the PTV. The exposure dose was established such that the dose at 95% volume of the PTV curve in DVH for the treatment plan optimized calculation was 5 Gy. We verified the model for this treatment plan using an ionization chamber dosimeter (A1SI, Standard Imaging Inc., USA) and a cylindrical solid phantom (cheese phantom, TomoTherapy Inc., USA) (Fig.3). This phantom is a cylinder of 30 cm in diameter

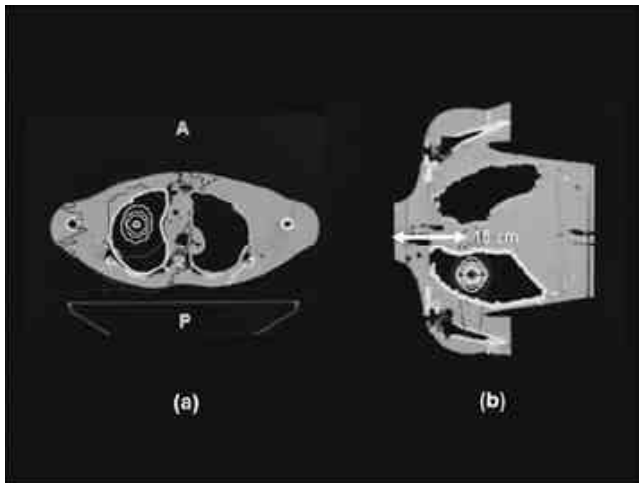


**Fig. 2.** A PTV position in the Rando-Phantom. (a) an axial and (b) an coronal CT images.

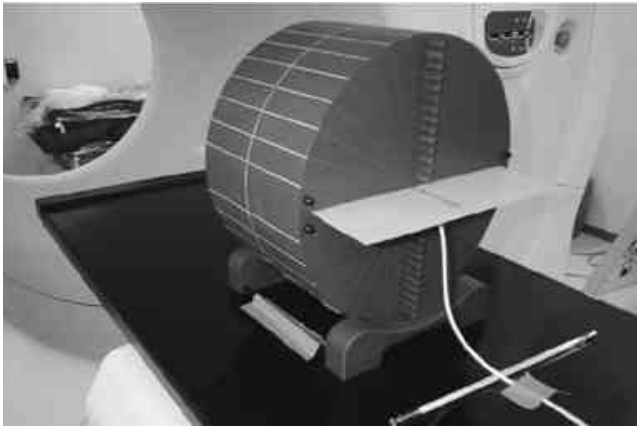


**Fig. 3.** Dedicated QA phantom used to verify the absorbed dose values acquired through the treatment plan optimization calculations for IMRT and the beam profile. The dose profile on the coronal plane is measured by EDR-2 film. Then, point absorbed dose is measured by a small ionization chamber detector. We start radiotherapy when the actual measurement value shows variance within 3% of the calculated value in the treatment plan.

and 18 cm in height. The phantom can be split in half from the central part, and the beam profile can be measured using EDR film. Also, there are holes for point dosimetry measurement, and the absorbed dose can be measured with an ionization chamber dosimeter. The absorbed dose as determined from actual measurements and the values from the optimized calculations for the treatment plan were compared in the region where the dose distribution inside the PTV was flat.

The absorbed dose of the peripheral organ was measured with a fluorescent glass dosimeter in the location of the left and right eyes, the thyroid, the left and right breasts, and the pelvic region. For this purpose, the florescent glass dosimeter was used in conjunction with an MIX-R<sup>14</sup> of 2 mm in thickness for the left and right eyes and a MIX-R of 1 cm in thickness for all other locations. The basic ingredients of MIX-R were polyisoprene, sulfur, zinc oxide, stearic acid and Nocceler CZ. The florescent glass dosimeters were used in a set of five, and evaluations were carried out using the mean value. The X-rays used in helical tomotherapy had energy of 6 MV, which approximates 1.25 MV cobalt gamma rays. Thus, a conversion was carried out for the acquired absorbed dose by using the following equation, where 1 Gy = 1 Sv:

$$H = D \cdot Q \cdot N.$$

Here,  $H$  is the patient dose [Sv],  $D$  is the absorbed dose [Gy],  $Q$  is the beam quality factor [ $Q = 1$  MV], and  $N$  is a correction factor [ $N = 1.0$ ]. The treatment beam parameters at time of exposure are shown in Table 1. In addition, to investigate the dose due to the change of dosimetry distance, we used a glass dosimeter to measure the relationship between the distance and dose. This measurement was performed in the same manner as the measurement of the absorbed dose at the phantom body. Dosimetry was performed at the points along the central axis at 10, 20, 30, 40 and 50 cm from the axial plane including PTV center.

**Table 1.** Exposure parameters used in optimization calculation for lung cancer treatment plan simulations.

Beam parameters				
Beam energy	Beam type	Exposure method	Beam on-time (s)	Absorbed dose of 95% in PTV
6 MV	Narrow slit beam	Helical therapy	1046.5	5 Gy
IMRT				

## Results

The measured doses were 3.13 mGy for the left lens and 3.22 mGy for the right lens. These doses were less than 0.1% of the established dose of 95% PTV at 5 Gy. The thyroid received a dose of 13.26 mGy (0.27% of the PTV dose), which was an exposure dose of approximately 4 times higher than the dose received by the lenses, owing to the proximity of the thyroid to the PTV.

The left and right breasts, which were on the trajectory of the helical tomotherapy, received doses of 227.94 mGy and 371.90 mGy, respectively. This confirmed that the left breast on the non-treated side received an equivalent of 4.6% of the PTV dose and the right breast on the treated side an equivalent of 7.4%. The pelvic region received a dose of 1.47 mGy, which was the lowest exposure dose among the target measurements, owing to its distance from the PTV. This represented less than 0.05% of the PTV dose.

The relation between the distance from the PTV and the dose is shown in Fig. 3. The dose is exponentially attenuated with increasing the distance from the PTV, 20 to 30

mGy at 10 cm, less than 10 mGy at 20 cm and around 2 mGy at 50 cm (Fig.4).

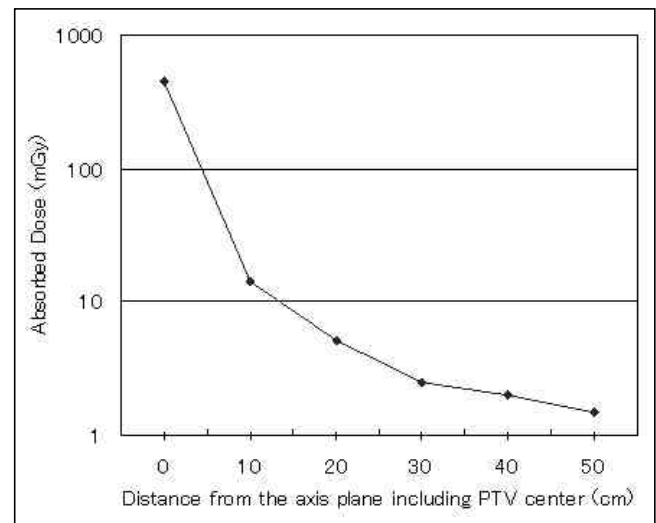


**Fig. 4.** Absorbed dose relation to the distance from the axis plane including PTV center.

**Table 2.** Absorbed dose for each position during helical tomotherapy treatment as measured with a fluorescent glass dosimeter.

organ	No. 1 rod	No. 2 rod	No. 3 rod	No. 4 rod	No. 5 rod	Mean dose <sup>a</sup> (mGy)	SD <sup>b</sup>
Right eye	3.08	3.17	3.20	3.29	3.34	3.22	0.10
Left eye	3.15	3.16	3.09	3.14	3.12	3.13	0.03
Thyroid	13.35	12.75	13.16	13.17	13.85	13.26	0.40
Right breast <sup>c</sup>	292.90	350.40	395.50	389.90	430.80	371.90	52.57
Left breast <sup>c</sup>	235.60	243.20	239.60	202.50	218.80	227.94	17.02
Pelvic area	1.44	1.57	1.44	1.46	1.43	1.47	0.06

<sup>a</sup>A group of five fluorescent glass dosimeters was used for each position of the phantom and the absorbed dose (mGy) was calculated as the mean.

<sup>b</sup>SD: standard deviation

<sup>c</sup>Right and left breast are in direct radiation field areas.

## Discussion

This study confirmed that the off-trajectory dose in helical tomotherapy can be sufficiently low. However, for peripheral organs on the trajectory of the helical tomotherapy, caution and validation are necessary in accordance with the exposure dose, although this also depends on the type and position of the peripheral organ and whether the treatment is single-dose or total dose.

Concerning the measurement of off-axis doses in helical tomotherapy, Ramsey et al. have reported results measured using a human-body phantom and a Thermo Luminescence Dosimeter (TLD)<sup>7</sup>. They consider an off-axis increase of leakage dose to be possible because the exposure time for treatment is from 5 to 15 minutes for IMRT by helical tomotherapy, which is longer than treatment using conventional linear accelerators. For that reason, they used an identical human-body phantom and carried out measurements of absorbed dose with a TLD under the same conditions using helical tomotherapy and a general linear accelerator. In that study, they found the highest dose to be  $1 \times 10^{-4}$  Sv/s and the lowest dose to be  $1 \times 10^{-6}$  Sv/s for treatment times of 120 to 600 seconds. Although dependent on factors such as the measurement location and phantom, this maximum value is similar to the breast dose (maximum value) that we measured. In comparison with IMRT using a general linear accelerator, the off-axis dose of helical tomotherapy was equal or lower, irrespective of its longer exposure time. They attributed this to the special construction of the shielding structure of the helical tomotherapy system.

In the present study, the actual measurement was 13.26 mGy when PTV (planning target volume) was 5Gy. Therefore, it becomes 132.6mGy, 10 times as much as the measurement, if the total dosage for radiotherapy is 50Gy; however, it is not clear from reports to date whether this dose can definitely increase the risk of thyroid cancer. Recent studies, showed that thyroid cancer can be induced by relatively low dose of radiation. In a follow-up survey of the atomic bomb survivors at Hiroshima and Nagasaki, thyroid cancer was more likely to occur in younger subjects, which was not observed in subjects over the age of 40. However, a causal relation with radiation exposure was not established<sup>15</sup>. Pacini et al. reported that thyroid cancer is clearly increasing at a greater rate in individuals exposed to radioactivated iodine in childhood due to the fallout of the Chernobyl incident in comparison with non-exposed individuals. Taking into account the possibility of increased risk of thyroid cancer in young children, the dose to the thyroid should be

minimized by implementing an optimal treatment plan<sup>16</sup>.

Day et al. investigated ophthalmologic disorders in individuals exposed to the fallout of the Chernobyl incident, to evaluate the relation between contamination due to the incident and cataracts. The participants in the study were approximately 1000 people who lived in the contaminated region and were under the age of 12 at the time of the incident and approximately 800 people who lived in a scarcely contaminated region. Based on the results of this study, posterior capsule opacification was found to be significantly increased in the contaminated region<sup>17</sup>.

In the research of Worgel et al., ophthalmological examinations were carried out in 1998 and 2000, targeting approximately 8000 cleanup workers living in five provinces in Ukraine. The odds ratio for posterior capsule opacification and type 1 cortical opacity increased with contamination with a threshold to be between 0.3 and 0.5 Gy, suggesting a far lower likelihood than values previously considered<sup>18</sup>. Chumak et al. studied problems relating to the validity of the reported doses used in the research of Worgel et al. and the evaluation of the beta rays. As a result, the dose to the crystalline lens for the majority of workers was found to be 100-200 mGy with a small proportion exceeding 500 mGy<sup>19</sup>. Moreover, as a result of re-examining 730 survivors of the Hiroshima and Nagasaki atomic bombs, Neriishi et al. reported that the point estimation for the threshold dose was 0.6 Sv for cortical cataracts (95% confidence interval [CI], <0.0-1.2 Sv), and 0.8 Sv for posterior capsule opacification (95% confidence interval [CI], <0.0-2.8 Sv)<sup>20</sup>. This falls far under the 5 Gy threshold for cataracts proposed in the 60th publication of the International Commission on Radiological Protection (ICRP)<sup>21</sup>.

Considering that the lower limit of the lens dose reported by Worgel et al. was 0.3 Sv, the lens dose measured in the present research was far lower than this threshold. However, in the case that the distance between the PTV and the lens was less than 5 cm, the dose to the lens became approximately 0.2-0.3 Sv; therefore, a custom block should be used to reduce exposure to the lens.

In the present research, the dose to the pelvic region was 1.72 mGy. This value became 17.2 mGy in the case that the total dose of the PTV was 50 Gy. This value is exceedingly low in comparison with the threshold dose at which sterility or an effect on embryos arises (ICRP recommended values).

Mammary glands are within the path of the therapeutic beams, and the dose in this study is 227.94 to 371.90 mGy. Regarding this point, when the total radiotherapy dosage is 50 Gy, the dose to mammary glands is approximately 2 to

4 Gy. Increased breast cancer was recognized more than ten years after the exposure to radiation. It has been shown that its risk is higher in females exposed to radiation at young ages than in those exposed at the age of 40 or more. In particular, exposure at the age of less than 20 has the highest risk<sup>22,23</sup>. The age of onset agrees with the age of high incidence of usual breast cancer, and differences in tissue types and so on that characterize radiation-induced breast cancer are not recognized between high-dose exposure, low-dose exposure, and no exposure. Although significant increase in incidence risk of bilateral breast cancer is not recognized, it is suggested that the risk may be high when the age of exposure is less than 20<sup>24</sup>. The dose to mammary gland in atomic bomb victims is estimated to be 0 to 6 Gy (0 to 6.08 Sv, average 0.276 Sv), and it is shown that incidence of breast cancer increases almost linearly with the exposed dose<sup>25</sup>.

On the other hand, influence of exposure to radiation in the cases of a low dose, a low dose rate, or a low dose rate with a high dose is not clarified scientifically. Therefore, for influence of low-dose exposure, the risk is estimated by model analyses based on the assumption that no threshold exists and that there exists a dose-response relation similar to that in the high-dose exposure, namely, cancer occurs stochastically in correlation with the total dose. However, we need to notice that the estimation methods are not well established and the results contain uncertainty. In fact, the linear dose-response relation is not confirmed even in atomic bomb victims below 0.25 Gy (average 0.17 Sv), and increase in incidence risk of contralateral breast cancer due to breast irradiation after breast-conserving surgery is also not recognized<sup>26,27</sup>.

From these facts, it is necessary to reduce the dose to mammary gland as much as possible. To realize it, remedies such as setting direction of radiation beam to avoid mammary gland tissues should be examined.

## Conclusions

In this research, we measured the exposure dose of the peripheral organs during helical tomotherapy IMRT with a fluorescent glass dosimeter. It was confirmed that the exposure dose reached a maximum value on the PTV trajectory and decreased in proportion to distance. Using the lung cancer model, the exposure dose to the left and right lenses was confirmed to be acceptable. However, when the distance from the PTV is less than 5 cm, a custom block should be used in order to reduce the dose to the lens.

## References

1. Burman C, Chui CS, Kutcher G et al. Planning, delivery, and quality assurance of intensity-modulated radiotherapy using dynamic multileaf collimator: a strategy for large-scale implementation for the treatment of carcinoma of the prostate. *Int J Radiat Oncol Biol Phys* 39(4):863-73, 1997
2. Sauer OA, Shepard DM, Mackie TR. Application of constrained optimization to radiotherapy planning. *Med Phys* 26(11):2359-66, 1999
3. Watanabe Y. Point dose calculations using an analytical pencil beam kernel for IMRT plan checking. *Phys Med Biol* 46(4):1031-8, 2001
4. Low DA, Chao KS, Mutic S, Gerber RL, Perez CA, Purdy JA. Quality assurance of serial tomotherapy for head and neck patient treatments. *Int J Radiat Oncol Biol Phys* 42(3):681-92, 1998
5. Low DA, Mutic S, Dempsey JF et al. Quantitative dosimetric verification of an IMRT planning and delivery system. *Radiother Oncol* 49(3):305-16, 1998
6. Kapulsky A, Gejerman G, Hanley J. A clinical application of an automated phantom-film QA procedure for validation of IMRT treatment planning and delivery. *Med Dosim* 29(4):279-84, 2004
7. Ramsey C, Seibert R, Mahan SL, Desai D, Chase D. Out-of-field dosimetry measurements for a helical tomotherapy system. *J Appl Clin Med Phys* 24;7(3):1-11, 2006
8. Araki F, Moribe N, Shimonobou T, Yoshiura T, Ikegami T, Ishidoya T. A study for narrow beam dosimetry using a radiophotoluminescent glass rod dosimeter [in Japanese]. *Japanese Journal of Radiological Technology* 60(7):939-947, 2004
9. Mackie TR, Balog J, Ruchala K et al. Tomotherapy. *Semin Radiat Oncol* 9(1):108-17, 1999
10. Mavroidis P, Stathakis S, Gutierrez A, Esquivel C, Shi C, Papanikolaou N. Expected clinical impact of the differences between planned and delivered dose distributions in helical tomotherapy for treating head and neck cancer using helical megavoltage CT images. *J Appl Clin Med Phys* 21;10(3):2969, 2009
11. Kissick MW, Mackie TR, Jeraj R. A delivery transfer function (DTF) analysis for helical tomotherapy. *Phys Med Biol* 7;52(9):2355-65, 2007
12. Kron T. Thermoluminescence dosimetry and its applications in medicine--Part 2: History and applications. *Australas Phys Eng Sci Med* 18(1):1-25, 1995
13. Thilman C, Adamietz IA, Ramm U et al. In vivo dose increase in the presence of dental alloys during 60Co-gamma-ray therapy of the oral cavity. *Med Dosim* 21(3):149-54, 1996
14. Ichirou Y. A New Flexible Water-Equivalent Material. *Jpn J Radiol* 36(2):143-7, 1975
15. Imaizumi M, Usa T, Tominaga T et al. Radiation dose-response relationships for thyroid nodules and autoimmune thyroid diseases in Hiroshima and Nagasaki atomic bomb survivors 55-58 years after radiation exposure. *JAMA* 1;295(9):1011-22, 2006
16. Pacini F, Vorontsova T, Demidchik EP et al. Post-Chernobyl thyroid carcinoma in Belarus children and adolescents: comparison with naturally occurring thyroid carcinoma in Italy and France. *J Clin Endocrinol Metab* 82(11):3563-9, 1997
17. Day R, Gorin MB, Eller AW. Prevalence of lens changes in Ukrainian children residing around Chernobyl. *Health Phys* 68(5):632-42, 1995
18. Worgul BV, Kundiye YI, Sergiyenko NM et al. Cataracts among Chernobyl clean-up workers: implications regarding permissible eye exposures. *Radiat Res* 167(2):233-43, 2007
19. Chumak VV, Worgul BV, Kundiye YI et al. Dosimetry for a study of low-dose radiation cataracts among Chernobyl clean-up workers. *Radiat Res* 167(5):606-14, 2007
20. Neriishi K, Nakashima E, Minamoto A et al. Postoperative cataract cases among atomic bomb survivors: radiation dose response and threshold. *Radiat Res* 168(4):404-8, 2007
21. Mountford PJ, Temperton DH. Recommendations of the International

- Commission on Radiological Protection (ICRP) 1990. *Eur J Nucl Med* 19(2):77-9, 1997
22. Tokunaga M, Land CE, Yamamoto T, Asano M, Tokuoka S, Ezaki H, et al. Incidence of female breast cancer among atomic bomb survivors, Hiroshima and Nagasaki, 1950-1980. *Radiat Res.* 112 : 243-72, 1987
23. Tokunaga M, Land CE, Tokuoka S, Nishimori I, Soda M and Akiba S. Incidence of female breast cancer among atomic bomb survivors, 1950-1985. *Radiat Res.* 138 : 209-23. 1994
24. Land CE, Tokunaga M, Koyama K, Soda M, Preston DL, Nishimori I, et al. Incidence of female breast cancer among atomic bomb survivors, Hiroshima and Nagasaki, 1950-1990. *Radiat Res.* 160 : 707-17. 2003
25. Thompson DE, Mabuchi K, Ron E, Soda M, Tokunaga M, Ochiaiubo S, et al. Cancer incidence in atomic bomb survivors. Part II : Solid tumors, 1958-1987. *Radiat Res.* 137 : S17-67. 1994
26. Veronesi U, Cascinelli N, Mariani L, Greco M, Saccozzi R, Luini A, et al. Twenty-year follow-up of a randomized study comparing breast-conserving surgery with radical mastectomy for early breast cancer. *N Engl J Med.* 347 : 1227-32. 2002
27. Poggi MM, Danforth DN, Sciuto LC, Smith SL, Steinberg SM, Liewehr DJ, et al. Eighteen-year results in the treatment of early breast carcinoma with mastectomy versus breast conservation therapy : the National Cancer Institute Randomized Trial. *Cancer* 98 : 697-702. 2003

